arXiv:cond-mat/0409668v1 [cond-mat.mtrl-sci] 24 Sep 2004

Understanding of the phase transformation from fullerite to amorphous carbon at the microscopic level

M. Moseler,[1] H. Riedel,[1] P. Gumbsch,[1] J. Stäring,[2] and B. Mehlig[2]

[1]*Fraunhofer-Institut für Werkstoffmechanik IWM, Wöhlerstr. 11, 79108 Freiburg, Germany*
[2]*Theoretical Physics, Göteborg University/Chalmers, Sweden*

(Dated: February 2, 2008)

We have studied the shock-induced phase transition from fullerite to a dense amorphous carbon phase by tight-binding molecular dynamics. For increasing hydrostatic pressures P, the C_{60}-cages are found to polymerise at $P < 10$ GPa, to break at $P \sim 40$GPa and to slowly collapse further at $P > 60$ GPa. By contrast, in the presence of additional shear stresses, the cages are destroyed at much lower pressures ($P < 30$ GPa). We explain this fact in terms of a continuum model, the snap-through instability of a spherical shell. Surprisingly, the relaxed high-density structures display no intermediate-range order.

PACS numbers: 61.48.+c, 62.25.+g, 64.70.Nd, 02.70.Ns, 62.50.+p

Rapid development in cluster science and nanotechnology has fostered the hope that materials exhibiting novel properties due to the existence of intermediate-range order (IRO) can be constructed from clusters [1] or nanotubes [2] as building blocks. Fullerenes (C_{60} molecules) represent one of the rare species of clusters available in macroscopic quantities [3]. It is not surprising, therefore, that fullerene-assembled materials have been studied for at least a decade now [4].

The extraordinary elastic properties of the molecular cage of C_{60} have inspired many to speculate about new carbon modifications with extraordinary mechanical performance [5]. Indeed, in early experiments very hard and stiff materials were synthesised (stable under ambient conditions) by compressing fullerite under high pressure [6]. Subsequently, these phases have been characterised experimentally by determining their structural, mechanical, and optical properties [7, 8, 9, 10, 11, 12, 13, 14, 15] revealing a plethora of ordered (polymerised fullerenes) and disordered (amorphous) carbon phases (see [7] for a review).

Based on electron diffraction experiments, shock-compressed fullerite [16], has been conjectured to be a *new form of amorphous diamond* exhibiting IRO [7]. Furthermore, it has been argued that the mechanical properties are determined by remnants of (partially) intact fullerene cages distinguishing these phases from tetrahedrally coordinated amorphous carbon (ta-C) produced by ion-beam techniques.

However, up to now, conjectures concerning the structural properties are based on indirect information; neither the process of formation of such structures nor the nature of the proposed intermediate range order is understood microscopically. Pioneering molecular-dynamics (MD) simulations have shown that subjecting fullerite to high pressure and high temperatures may give rise to a dense amorphous phase [17]. However, the sample in [17] had to be compressed to very high densities (4.4 g/cm^3 at $T = 2500$K) corresponding to pressures exceeding 100GPa, far beyond any experimentally obtainable conditions. Empirically, the transition from fullerite to amorphous carbon occurs in the range of $10 - 30$ GPa, depending on the speed of compression and on temperature (room temperature in [6] and approximately 2000K in shock experiments [7, 16]). How may this contradiction be resolved? There are indications that shear stress may play a role in the destabilisation of the cages [6]. However, at present it is not known which microscopic processes cause the transition from fullerite to amorphous carbon.

There is thus a pressing need for a theoretical understanding of the exact microscopic mechanisms occurring during this phase transition. To which extent is a macroscopic picture of a rapidly imploding spherical shell appropriate? Is shear important? How strong is the dependence of the final structural properties on the details of the compression process? Is there intermediate range order in the final dense carbon phase?

This letter reports on quantum-mechanical computer simulations of shock-compressed fullerite, starting from fcc-crystallised and tetragonally polymerised fullerenes. Our findings provide profound insights into the above-mentioned issues and can be summarised as follows.

Microscopic mechanisms and transition pressure. Hydrostatic pressures transform fullerite into amorphous carbon by a succession of three steps: *(i)* polymerisation mainly by 2+2 ring-formation starting at $P < 10$ GPa, *(ii)* breaking of the C_{60} cages starting at $P \sim 40$ GPa, and *(iii)*, at still higher pressures, collapse of the broken C_{60} cages via formation of chemical bonds across the cage. Remarkably, process *(iii)* occurs very slowly, and (c.f. Ref. [17]) very high hydrostatic pressures (exceeding 60 GPa) are required for a complete collapse.

Non-hydrostatic (external) stresses, by contrast, result in a rapid shear deformation of the unit cell: steps *(ii)* and *(iii)* happen simultaneously and very rapidly. In other words, the C_{60} molecules are ground – and not merely crushed to form amorphous carbon. Application

of shear significantly lowers the transition pressure. We explain this fact in terms of a continuum model (snap-through instability of a spherical shell under shear).

Microstructure and intermediate-range order. We analyse the resulting structures after compression to 35 GPa and subsequent relaxation to ambient conditions and find that the morphology depends on the amount of applied shear. In order to characterise the phase transition and resulting morphologies it is not sufficient to merely specify pressure and temperature, shear is equally important. At low shear stresses the mechanical strength of the material is low and at the same time, intact C_{60} cages are still present. At high shear stresses, by contrast, no remnants of C_{60} cages are observed. In this case, bulk moduli are found to be large, of the order of that of diamond. The radial distribution functions $G(r)$ indicate that our fullerite-derived dense phase has lost its nanoscopic order and turned into conventional ta-C. We show that fine details in $G(r)$ of shock compressed fullerite [16] are most likely effects of an incomplete experimental k-space sampling and not a fingerprint of IRO.

Methods. We simulate the MD of shock-compressed fullerite within an fcc and a tetragonal unit cell containing four and two C_{60}, respectively. Interatomic forces are determined within a non-orthogonal density-functional-based tight-binding scheme [18]. A Langevin thermostat is used to keep the temperature close to the 2000 K reported for shock conditions [7]. Spontaneous shearing of the simulation cell is allowed for and external shear stresses were applied by using a Rahman-Parrinello [19] barostat. After thermalisation of the sample, the external pressure is increased linearly from 0 to 70 GPa within 100 ps. Bond formation and breaking as well as sp^3/sp^2 hybridisation is determined based on a population analysis of the bond orbitals, similar to the Mulliken charge analysis [20]. In the remainder of this letter we explain how the results summarised above follow from our simulations (Figs. 1 to 3).

Hydrostatic conditions. Fullerite proves to be very stable under isotropic compression, withstanding high pressures. The microscopic mechanism of collapse is apparent from Fig. 1a displaying the evolution of inter- and intramolecular bonds and the representative fate of one of the cages. Starting from an fcc-ordered crystal, the structure changes gradually through polymerisation of C_{60}-molecules (see the rise in the number intermolecular bonds for $P > 5$ GPa, lower curve of Fig. 1a). Double bonds in neighbouring cages break and rehybridise with each other to form a mainly four-membered rings (2+2 cycloaddition [21, 22]). This process is completed for $P > 26$ GPa and the number of intermolecular bonds stays constant up to $P_c = 38$ GPa (Fig. 1a).

Upon increasing the pressure beyond $P_c = 38$ GPa, the cages break (inset in Fig. 1a), indicated by a drop in the number of intramolecular bonds (upper curve in Fig. 1a) and form new bonds to neighbouring fullerenes

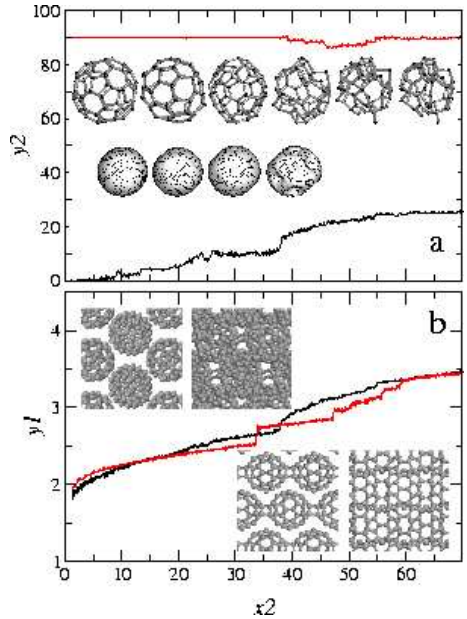

FIG. 1: Fullerite under increasing hydrostatic pressure, at 2000 K. **a** Evolution of bonding in the absence of shear stress, starting from an fcc crystal of fullerenes. Shown are the number of bonds per C_{60}-molecule as a function of applied pressure. Intramolecular (red, upper curve) and intermolecular bonds (black, lower curve) are plotted separately. Insets show the shapes of a representative C_{60} molecule as the pressure increases, in steps of 14 GPa, and the results of a continuum model (snap-through instability of a spherical shell) at pressures $5, 20, 30$ and 40 GPa. The instability occurs between the third and fourth configurations. **b** Comparison of density evolution of the compressed C_{60} crystal starting from the fcc (black curve) and from a tetragonally polymerised phase (red curve). Insets show the initial and a intermediate configurations (at pressures 0 and 35 GPa, respectively) for the fcc (top row) and tetragonal (bottom row) phase.

(sudden raise of the lower curve in Fig. 1a) leading to a densification of the material (Fig. 1b). At even higher pressures, the C_{60} cages gradually collapse forming bonds inside the cages marked by a steady increase in the number of intramolecular bonds in Fig. 1a for large values of P. When and how fast this process occurs depends on the local alignments of the cages.

In order to study the influence of the initial configuration on the phase transition, a second simulation starting from a tetragonally polymerised state (lower inset in Fig. 1b) has been performed. The resulting density-pressure curve (Fig. 1b) is qualitatively unchanged at high pressures, as is the resulting structure (at pressures exceeding 60 GPa). In the intermediate regime, however, the structures are quite different (insets of Fig. 1b), as are the density-pressure curves (Fig. 1b): in the tetragonal phase, the C_{60} molecules cannot rotate freely (as opposed to those in fcc phase). Intermediate configurations are thus seen to be very regular, with a high degree of polymerisation.

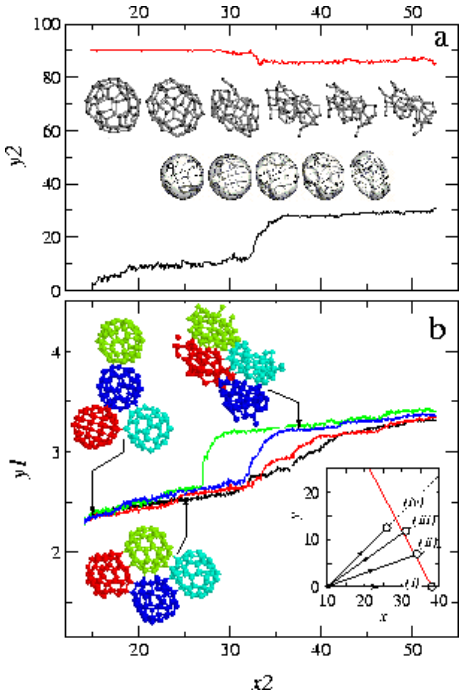

FIG. 2: Fullerite compressed in the presence of external shear. **a** Evolution of the number of bonds per C_{60} molecule (color coding as in Fig. 1a). Insets displays the morphology of a C_{60}-molecule (top) as the pressure increases, in steps of 6 GPa, and from a continuum model (bottom). **b** Density as a function of pressure in the presence of external shear $S = \sigma_{xy}$. Shown are four plots corresponding to four pathways in the S-P-plane as given in the inset: *(i)* black, *(ii)* red, *(iii)* blue, *(iv)* green. Locations of the collapse transition are shown as points in the S-P-plane. Also shown is the critical line (red) as determined from a continuum model. Finally, morphologies of the C-atom configurations in a unit cell for case *(iii)* are also shown.

Regardless of the initial conditions, unrealistically high pressures (exceeding 60 GPa) are required to entirely destroy the cages (resulting in a dense amorphous phase after relaxation to ambient conditions). This is not consistent with the experimentally found transition pressures.

Non-hydrostatic conditions. We have compressed the polymerised fcc phase under non-hydrostatic conditions, along three paths - *(ii)*, *(iii)*, and *(iv)* - in the S-P plane shown in the inset of Fig. 2b ($S = \sigma_{xy}$ is the shear stress in the (001) plane). Path *(i)* corresponds to the hydrostatic case. Fig. 2a shows the numbers of intra- and intermolecular bonds per C_{60} molecule, for case *(iii)*. Comparison with Fig. 1a and inspection of the pressure-density relationship in Fig. 2b confirms that shear plays an important role lowering the critical pressure and increasing the speed of the phase transition which happens now within a few GPa at approximately 34, 31, and 26 GPa for cases *(ii)*, *(iii)*, and *(iv)*. The critical shear values at the collapse are $S_c = 6.94, 11.8$ and 12.5 and shown as points in the S-P-plane in Fig. 2b.

Load mode	ρ [g/cm^3]	B [GPa]	% sp^3
(i)	2.1	50	18%
(ii)	2.3	60	20%
(iii)	3.0	210	69%
(iv)	3.1	320	79%

TABLE I: Characterisation of fullerite phases after compression to 35 GPa and relaxation to ambient conditions. Load conditions as in Fig. 2b.

Fig. 2a also indicates that the microscopic mechanism is different from the zero-shear case described above: in the presence of shear the cages are ground (see the transition from a spherical to an oblate cluster in the inset of Fig. 2a). After a rapid transition the number of intra- and intermolecular bonds remains constant (as opposed to Fig. 1a). The cages are so strongly flattened that the number of intramolecular bonds cannot be increased by raising the pressure further.

The final structure however (at pressures > 35 GPa) is similar to the structure obtained under hydrostatic conditions at pressures exceeding 60 GPa.

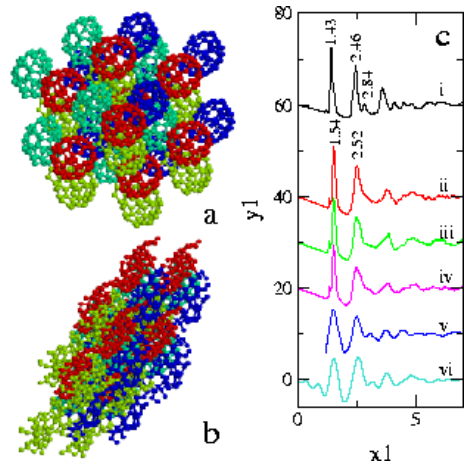

FIG. 3: Structures of fullerite relaxed from from P=35 GPa,T = 2000 K to ambient conditions. **a-b** morphologies of the fcc unit cells resulting from compression with two different shear values: (a) no shear and (b) shear according to path *(iv)* in the S-P-plane displayed in Fig. 2b. **c** radial distribution function $G(r)$ averaged over 20 ps along a trajectory at ambient conditions: (**i**) sample after a hydrostatic compression to $P = 35$ GPa, (**ii**) same compression but with high shear, (**iii**) reference sample without any intermediate range order (see text), (**iv**) after hydrostatic compression to $P = 60$ GPa, (**v**) experimental G(r) of shock-treated fullerite [16], (**vi**) same curve as in **ii**, convolved with a peak-shape function $\sin(Qr)/(\pi r)$ with $Q = 12.0$Å^{-1}.

A continuum model. To which extent can the phase transition in Figs. 1 and 2 be understood in terms of a continuum model? We have modeled a C_{60}-molecule in fullerite as a spherical shell with diameter 0.71nm.

Its Young modulus (5.32 TPa) and effective thickness (0.08nm) are determined from tight-binding simulations of a graphene sheet. Forces are applied at 12 nodes corresponding to the fcc symmetry of the fullerite crystal. The shell exhibits a snap-through instability at $P_c = 37.8$ GPa (see snapshots of the shell in Fig. 1a) to be compared with 38 GPa obtained above. It must be noted that the agreement is better than expected [23], and that the continuum model cannot explain the dynamics and morphologies at pressures beyond the collapse (see below).

The decrease of the critical pressure with increasing shear stress can also be understood in terms of the continuum model (inset of Fig. 2a): shear destabilises a spherical shell under pressure and lowers the critical pressure. The continuum model predicts that critical shear stress and pressure are linearly related, the result is shown as a red line in the inset of Fig. 2b, in good agreement with the atomistic results for not too large values of shear stress. This shows that the onset of the instability of fullerite under shear stress can be described by elasticity theory. The ensuing collapse, however, must be modeled microscopically (in terms of breaking of bonds and rehybridisation). Finally, the continuum model fails at high shear stresses (c.f. path *(iv)* in the inset of Fig. 2b).

Resulting morphologies. The question remains: what structures are obtained when the compressed fullerites are relaxed from – for instance – 35 GPa and 2000 K to ambient conditions? The morphology of the relaxed phase depends clearly on the amount of applied shear. Consider the relaxed structures shown in Fig. 3a and b. They were obtained from samples compressed along the S-P-path *(i)* and *(iv)* (as shown in the inset of Fig. 2b), respectively. For no or low shear stress, densities, bulk moduli and sp^3 fractions are small (see load mode *(i)* and *(ii)* in Tab. 1), polymerisation is evident but the cages are still intact (Fig. 3a). At high shear (load mode *(iii)* and *(iv)* in Tab. 1), by contrast, densities, bulk moduli and sp^3 fractions are much larger and no remnants of C_{60} cages are found (Fig. 3b).

Does the radial distribution function reflect possible IRO in the relaxed samples? Curves **i** and **ii** in Fig. 3c display $G(r)$ for the two cases discussed above. In the zero-shear case, C_{60}-specific distances are still present (the average nearest-neighbour bond length in graphite is 0.142 nm) thus showing clear evidence of IRO. In the other sample, by contrast, the radial distribution function is clearly different exhibiting the first peak at 0.154 nm, as in diamond. Curve **iii** in Fig. 3c corresponds to a sample relaxed from $P = 60$ GPa, $S = 0$ GPa to ambient conditions. Obviously this phase has a structure similar to **ii**.

To test the hypothesis of a *new form of amorphous diamond*, we have created reference sample exhibiting no IRO, obtained by isochorus heating of 240 carbon atoms to 10000 K while monitoring the system for sufficient chaotic motion followed by a relaxation to ambient conditions. It exhibits ta-C characteristics and approximately the same density and sp^3/sp^2 hybridisation as the densest structure in Tab. 1 Surprisingly, the resulting $G(r)$ (curve **iv** in Fig. 3c) is essentially identical to **ii** and consequently, the radial distribution function **ii** in Fig. 3b provides no fingerprint of IRO.

The conditions of the simulations reported here are close to those in the shock-compression experiments reported in ref. [16]. The third peak in the empirically determined $G(r)$ (curve **v** in Fig. 3c) at approximately 0.312 nm has been accredited to the diameter of six-membered rings in the C_{60} molecules or to a slightly elongated third-neighbor distance for diamond. However, it should be kept in mind that experimental radial-distribution functions are generated from reciprocal space scattering information which is limited by an inevitable momentum cut-off Q. Thus, for the sake of comparability, the simulated $G(r)$ of our dense amorphous carbon (curve **ii**) was convoluted with an appropriate cut-off function reflecting the experimental Q=12 Å^{-1} [16]. The resulting radial distribution function (curve **vi** in Fig. 3c) is very similar to that observed in [16]. We conclude that the third peak in **v** is unlikely to reflect IRO, it is likely to be an effect of the finite experimental resolution.

Support from the Fraunhofer MAVO MMM-Tools and Vetenskapsrådet is gratefully acknowleged. We thank T. Frauenheim for his Hydrocarbon-Slater-Koster tables. Computations were performed on the CEMI cluster of the Freiburg Fraunhofer Institutes EMI/ISE/IWM.

[1] K. Sattler, ed., *Cluster assembled materials* (Trans Tech Publications, Zurich, 1996).
[2] J. A. Elliott et al., Phys. Rev. Lett. **92**, 095501 (2004).
[3] W. Krätschmer et al., Nature **347**, 354 (1990).
[4] M. Tachibana et al., Phys. Rev. B **94**, 14945 (1994).
[5] R.S.Ruoff and A.L.Ruoff, Nature **350**, 663 (1991).
[6] M. Nunez-Regueiro et al., Nature **354**, 289 (1991).
[7] V. D. Blank et al., Carbon **36**, 319 (1998).
[8] V. V. Brazhkin et al., Phil. Mag. A **82**, 231 (2002).
[9] F. Moshary et al., Phys. Rev. Lett. **69**, 466 (1992).
[10] J. Haines et al., Annu. Rev. Mater. Res. **31**, 1 (2001).
[11] V. V. Brazhkin et al., Phys. Rev. B **56**, 11465 (1997).
[12] V. V. Brazhkin et al., J. Appl. Phys. **84**, 219 (1998).
[13] R. A. Wood et al., J. Phys.: Condesn. Matter **14**, 11615 (2002).
[14] M. H. Manghnani et al., Phys. Rev. B **64**, 121403 (2001).
[15] M. Nunez-Regueiro et al., Phys. Rev. Lett. **74**, 278 (1995).
[16] H. Hirai et al., Phys. Rev. B **52**, 6162 (1995).
[17] B. L. Zhang et al., Europhys. Lett. **28**, 219 (1994).
[18] D. Porezag et al., Phys. Rev. B **51**, 12947 (1995).
[19] M. Parrinello and A. Rahman, Phys. Rev. Lett. **45**, 1196 (1980).
[20] M. Elstner et al., Phys. Rev. B **58**, 7260 (1998).
[21] A. Rao, Science **259**, 955 (1993).

[22] The polymerisation pattern depends on the rotational orientations of the cages and also on the compression speed. Of course, a lower compression rate allow the C_{60} molecules to relax through rotation forming a lower energy polymer.

[23] A C_{60}-cage consists of 5- and 6-rings whereas the elastic constants were taken to be those of a graphene sheet (consisting of 6-rings only).